

communications

earth & environment

ARTICLE



<https://doi.org/10.1038/s43247-022-00475-w>

OPEN

Sensitivity of subregional distribution of socioeconomic conditions to the global assessment of water scarcity

Prakat Modi¹✉, Naota Hanasaki¹, Dai Yamazaki³, Julien Eric Stanislas Boulange² & Taikan Oki¹

Water availability per capita is among the most fundamental water-scarcity indicators used extensively in global grid-based water resources assessments. Recently, it has extended to include the economic aspect, a proxy of the capability for water management which we applied globally under socioeconomic-climate scenarios using gridded population and economic conditions. We found that population and economic projection choices significantly influence the global water scarcity assessment, particularly the assumption of urban concentrated and dispersed population. Using multiple socioeconomic-climate scenarios, global climate models, and two gridded population datasets, capturing extremities, we show that the water-scarce population ranges from 0.32–665 million in the future. Uncertainties in the socioeconomic-climate scenarios and global climate models are 6.58–489 million and 0.03–248 million, respectively. The population distribution has a similar impact, with an uncertainty of 169.1–338 million. These results highlight the importance of the subregional distribution of socioeconomic factors for future global environment prediction.

¹Department of Civil Engineering, Graduate School of Engineering, The University of Tokyo, Tokyo, Japan. ²National Institute for Environmental Studies, Tsukuba, Japan. ³Institute of Industrial Science, The University of Tokyo, Tokyo, Japan. ✉email: prakatmodi@gmail.com

Water is vital for life on Earth. However, it is heterogeneously distributed over space and time¹. Over the past 100 years, the human water demand has increased 8-fold due to the quadrupling of the global population, increase in per-capita food demand, and higher standard of living^{2–8}. Socioeconomic development, together with ongoing climate change, has placed a burden on global freshwater resources and has caused an increase in water scarcity^{9,10}, which is determined primarily by the supply (availability) and demand (use) of water^{11–14}. Numerous indices have been devised and applied to assess the present and future global water resources at catchment, national, and global scales^{11,15,16}. Since 2000, such global assessment has been conducted in a grid-based manner, consistent with the advancement of hydrological modelling and global data development. Among the water scarcity indices, the availability of water per capita (APC) is the most fundamental and popular one.

Water scarcity is affected by economic conditions¹⁷ because the water supply depends on water management supported by infrastructure and technology (e.g., dam construction, desalination¹⁸, and virtual water imports or hidden flows of water embedded in food or other commodities imported through international trade¹⁹). The unavailability of water due to a lack of infrastructure or technology is termed economic water scarcity¹². The relationship between physical and economic water scarcity has been long debated; still, well-accepted indices or relationships have yet to be established. Oki et al.¹⁹ proposed a threshold line (equation) on the space of gross domestic product (GDP) per capita (horizontal axis) and APC (vertical axis) and found that no country is plotted below the line and hypothesised it as a universal empirical rule between two variables (hereafter hypothesis). Oki and Quiocho²⁰ examined the hypothesis on a grid basis of ~50 km (0.5°) for the present time using per capita GDP considering purchasing power parity (GDP-PPP) with the exchange rate of USD 2005. They found some locations facing both physical and economic water scarcity, which could only be seen at the subnational scale. Identifying such crucially vulnerable locations is essential to achieving international targets, including the Sustainable Development Goal Target 6.

Using the proposed methodology of Oki and Quiocho²⁰, we identified the locations and people facing survival difficulties at the beginning and end of the 21st century due to physical and economic water scarcity under climatic and social changes. We considered the latest grid-based socioeconomic data, i.e., GDP-PPP and various distribution of future gridded population, accounting urban concentrated (Murakami and Yamagata [hereafter MY19]²¹) and dispersed (Jones and O'Neill [hereafter JO16]²²) population, along with hydrological simulation output data. Our research questions were threefold. First, Does the hypothesis hold in the future at the country-scale? Second, Does the hypothesis hold in the future at the grid-scale? Third, How sensitive are results to the gridded socioeconomic scenarios used?

Results and discussion

Availability per capita. The APC water stress indicator represents the state of physical water scarcity. The total population under a certain level of water scarcity is called the stressed population. We calculated the water-stressed population and compared it to earlier estimates for validation. We found that the total population percentage (calculated using the ensemble mean discharge) facing acute physical water stress calculated using the APC of 500 m³/capita/year will vary as to 54.9^{+1.1%} (47.6^{-2.5%}), 66.6^{+2.8%} (59.8^{-3.3%}), and 55.6^{+4.2%} (47.0^{-2.6%}) (+/- values show the maximum variation considering discharge using single GCM to the ensemble mean discharge) at the end of the century

(i.e., the year 2099) under the SSP1-RCP2.6, SSP3-RCP7.0, and SSP5-RCP8.5 scenarios, respectively, representing different socioeconomic and climate conditions considering the MY19 (JO16) future population dataset (methods for scenarios and datasets details). By contrast, 44.5% (45.1%) of the global population faced acute physical water stress at the beginning of the century (i.e., the year 2000). The above percentages correspond to 3.5 (3.3), 7.9 (7.5), and 3.9 (3.4) billion populations for the SSP1-RCP2.6, SSP3-RCP7.0, and SSP5-RCP8.5 scenarios and 2.68 (2.75) billion for the historical scenario (i.e., beginning of the century). The historical value is consistent with the value of 2.7 billion previously reported by Hoekstra et al.¹³ and 2.4 billion mentioned by Oki and Kanae¹.

APC enhanced with GDP per capita—country-scale assessment. Next, we analysed the relationship between APC and GDP per capita. First, to revisit the findings of Oki et al.¹⁹, we conducted country-level analyses for the beginning (i.e., the year 2000) and end (i.e., the year 2099) of the century. To compare the absolute change for a longer period with the constant exchange rate, we used GDP-PPP per capita (USD 2005) due to its availability and defined water stress (physical and economic water scarcity) for both past and future scenarios using the same threshold line (see “Methods” section). The consistency in the results in terms of distribution of countries (Fig. 1 and Supplementary Fig. 1) for both historical (GPWv4 and HYDE3.2) and future (MY19 and JO16) population datasets confirm the similarity in aggregated country-level population data. We did not find any countries below the threshold line at the end of the

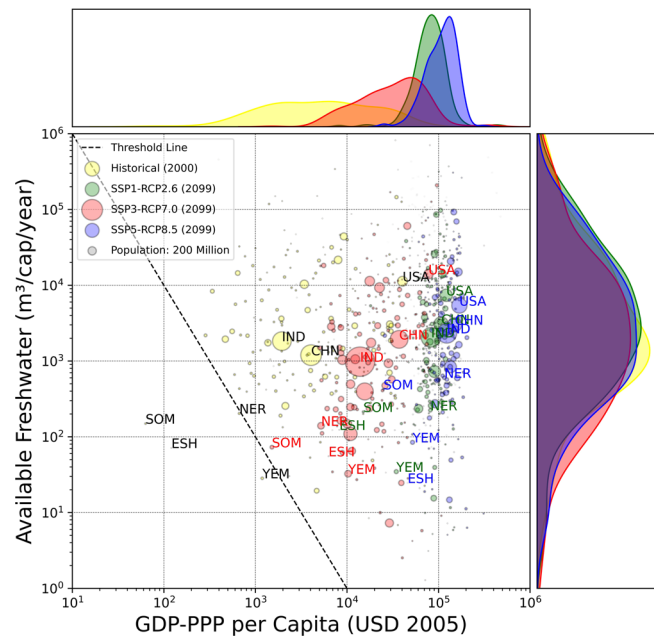


Fig. 1 Country-level scatter plot for APC vs GDP-PPP per capita and

density plot considering the number of countries for various socioeconomic and climate scenarios. Each circle corresponds to a country, and the circle's size corresponds to the country's population. CHN, ESH, IND, NER, SOM, USA, and YEM represent China, Western Sahara, India, Niger, Somalia, United States of America and Yemen, respectively. Yellow, green, red, and blue colours represent the historical, SSP1-RCP2.6, SSP3-RCP7.0, and SSP5-RCP8.5 scenarios, respectively, and the dashed line represents the threshold value for physical and economic water scarcity. The analysis was performed considering the GPWv4 dataset for the historical, i.e., the year 2000 population and MY19 for the future, i.e., the year 2099 population.

century, whereas we found Somalia, Western Sahara, Yemen, and Niger below the threshold line at the beginning of the century (Fig. 1, Supplementary Table 1 for base scenario experimental settings, results for other combinations of climate and population dataset are provided as Supplementary Fig. 1). The comparison of per capita water availability (APC) for countries below the threshold line for this study and additional analysis considering various climate forcing data with the same socioeconomic data showed substantial differences. These arid region countries have less runoff and considerable sensitivity towards the metrological data, causing the large difference in availability per capita (APC) of freshwater (Supplementary Table 2 for comparison of values considering different climate forcing data). Additionally, the quality of socioeconomic data contains uncertainty due to political instability^{23–26}, defying the hypothesis for these countries. We confirmed that although a few countries can contradict, the hypothesis of Oki et al.¹⁹ remains valid for various scenarios considered.

APC enhanced with GDP per capita—grid-scale assessment.

Next, we proceeded with grid-level analyses. We confirmed the existence of locations in the world facing the challenges of economic and physical water scarcity identified at 0.5° resolution (Fig. 2, results of SSP1–RCP2.6 and SSP5–RCP8.5 are shown in Supplementary Fig. 2 and Supplementary Fig. 3). The total population and spatial distribution facing challenges (i.e., grids below the threshold line defined by Eq. 1) differed in the different scenarios.

It can be observed from the density plots in Fig. 1 and Fig. 2 that there is a rightward shift in the peak and a significant increase in the mean and median values of the GDP-PPP per capita for the future scenarios compared to the historical scenario. The density plot for the APC for the future follows a trend similar to the trend of the past (i.e., a similar frequency distribution of APC at the grid scale), with an increase (decrease) in the median values observed for the future scenarios for MY19 (JO16) at the grid level (Supplementary Table 3 and Supplementary Table 4 for results of all statistical analyses considering future and historical datasets).

We calculated the population facing hardship due to both physical and economic water scarcity (i.e., grids below the threshold line defined by Eq. 1). As a result, at the end of the 21st century (i.e., the year 2099), $0.32^{+0.68}_{-0.00}$ (234^{+24}_{-10}) million people were estimated to face hardship under the SSP1–RCP2.6 scenario when using an urban-concentrated, i.e., MY19 (dispersed, i.e., JO16) population dataset. The estimated populations facing hardship under the SSP3–RCP7.0 and SSP5–RCP8.5 scenarios were 327^{+202}_{-35} (665^{+181}_{-67}) and $6.9^{+1.2}_{-1.1}$ (176^{+36}_{-3}) million respectively (+/- values show the maximum variation in the global population facing water scarcity, calculated considering discharge using single GCM and the ensemble mean discharge), compared to 327 (358) million at the beginning of this century (i.e., the year 2000) (Fig. 2e, Supplementary Table 5). Analysis considering MY19 and JO16 population datasets yield three orders of difference in the stressed population at maximum. The total number of water-stressed populations would decrease in the future (except for the SSP3–RCP7.0 with JO16 population distribution i.e., Future370–JO16 experiment) due to an increase in income.

Analysis considering various scenarios (Supplementary Table 1 for scenarios) shows that the uncertainty associated with the SSP–RCP scenarios (i.e., maximum, and minimum difference in the population facing scarcity considering any two scenarios among SSP1–RCP2.6, SSP3–RCP7.0, and SSP5–RCP8.5 for the ensemble mean discharge) and global climate models (GCMs) (i.e., maximum and minimum difference in the population facing

scarcity considering any two GCMs for a particular SSP–RCP scenario) were in the range of 6.58–489 and 0.03–248 million, respectively (Supplementary Table 5).

We found that the population distribution uncertainty (i.e., maximum and minimum difference in the population facing scarcity considering MY19 and JO16 gridded population distribution for a particular SSP–RCP scenario) for the end century (i.e., the year 2099) followed a similar trend and was in the range of 169.1–338 million (Supplementary Table 5). At the same time, the uncertainty at the beginning of the century (i.e., the year 2000) was within ~10 %, considering GPWv4 and HYDE3.2 gridded population datasets, confirming the high accuracy in estimation of historical population and their distribution. The maximum range value is brought by SSP3–RCP7.0, which is attributed to the large dispersion of population distribution in the SSP3. The grid-level analyses revealed that the future prediction includes large uncertainty due to the spatial distribution of within-country population along with the SSP–RCP paths of global sustainability (SSP1–RCP2.6), regional rivalry (SSP3–RCP7.0), and economic optimism (SSP5–RCP8.5) taken by the world (Fig. 3). The number of water-scarce grids (i.e., grids below the threshold line) in the future will increase or decrease compared to the past and depend mainly on the spatial distribution of population and GDP compared to freshwater availability.

Factor decomposition. The spatial distribution of grids below the threshold line of various historical and future scenarios (Fig. 3) showed that there would be an emergence of new water-scarce grids in the future, i.e., new grids facing water scarcity in future scenarios but were not facing water scarcity in the historical scenarios. These grids will face water scarcity either due to the decrease in freshwater availability (climate change) or GDP-PPP (socioeconomic change) or an increase in the population (socio-economic change) among the considered variables for the analysis. Fig. 4 presents the boxplot distributions of absolute values for freshwater (mm/year), population density (capita/km²), and GDP-PPP (USD/year) for newly identified water-scarce grids (grids facing scarcity in the future but not facing it in the past), comparing the values for the historical and future scenarios. The freshwater availability (mean and median values) does not change significantly over time for the new water-scarce grids, i.e., the difference between the future scenarios (SSP1–RCP2.6, SSP3–RCP7.0, and SSP5–RCP8.5) and the historical scenario is negligible. Compared to freshwater, there is a significant increase in population density for all considered scenarios and a less significant increase (decrease) of GDP-PPP of the grids (regions) for the MY19 (JO16) population datasets (Supplementary Table 6 for statistical analysis), suggesting that the primary reason for the water scarcity in these areas will be population growth.

The global water scarcity analysis considering various future scenarios (SSP1–RCP2.6, SSP3–RCP7.0, and SSP5–RCP8.5) identify various possible water stress regions (grids below the threshold line) of the world affecting the different number of populations. The common water-scarce grids recognised in all these scenarios (grids showing water scarcity for the SSP1–RCP2.6, SSP3–RCP7.0, and SSP5–RCP8.5 scenarios simultaneously) have the highest possibility (certainty) of facing water scarcity in the future. We compared the sensitivity analyses (methods for the approach adopted and Supplementary Table 7 for sensitive analysis experiment settings) results with the base scenario (Supplementary Table 1) values to know the major factor causing water stress among the considered variables for the grids with the highest possibility of water scarcity. The water-scarce population, which can be simultaneously identified in all future scenarios, will be in the range of 0.46–1.82 (156–393)

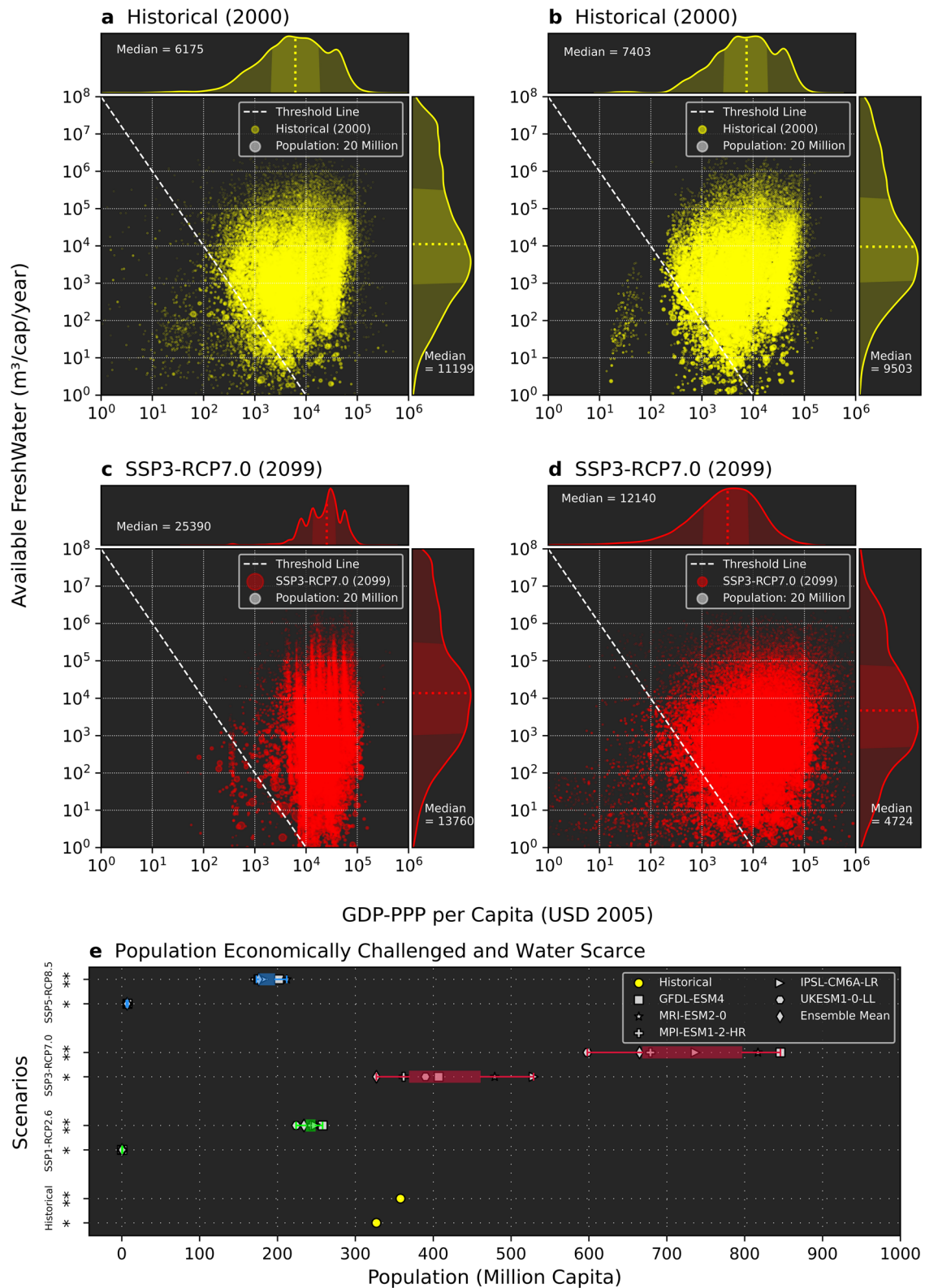


Fig. 2 Grid-level scatter plots for APC vs GDP-PPP per capita and density plot considering the number of grids. **(a)** Historical-GPW, **(b)** Historical-HYDE, **(c)** Future370-MY19, and **(d)** Future370-JO16 scenarios. Grid values are represented as circles, and the dashed line represents the threshold line proposed by Oki et al.¹⁹. The density plot includes dotted coloured lines (lime and red) for the median and dark shading for the interquartile range (first and third quartiles). The white circle represents the grid size of 20 million population. **(e)** Boxplot for the total population facing physical and economic water scarcity (grids below the threshold of Eq. 1) for all considered scenarios. Legend symbols represent the analysis using the discharge considering various GCMs and the ensemble mean of discharge considering all GCMs. *analysis for Historical-GPW and Future-MY scenarios, **analysis for Historical-HYDE and Future-JO scenarios (Supplementary Table 1 for scenarios/ experiment settings, and Supplementary Table 5 for water-scarce population and uncertainty values).

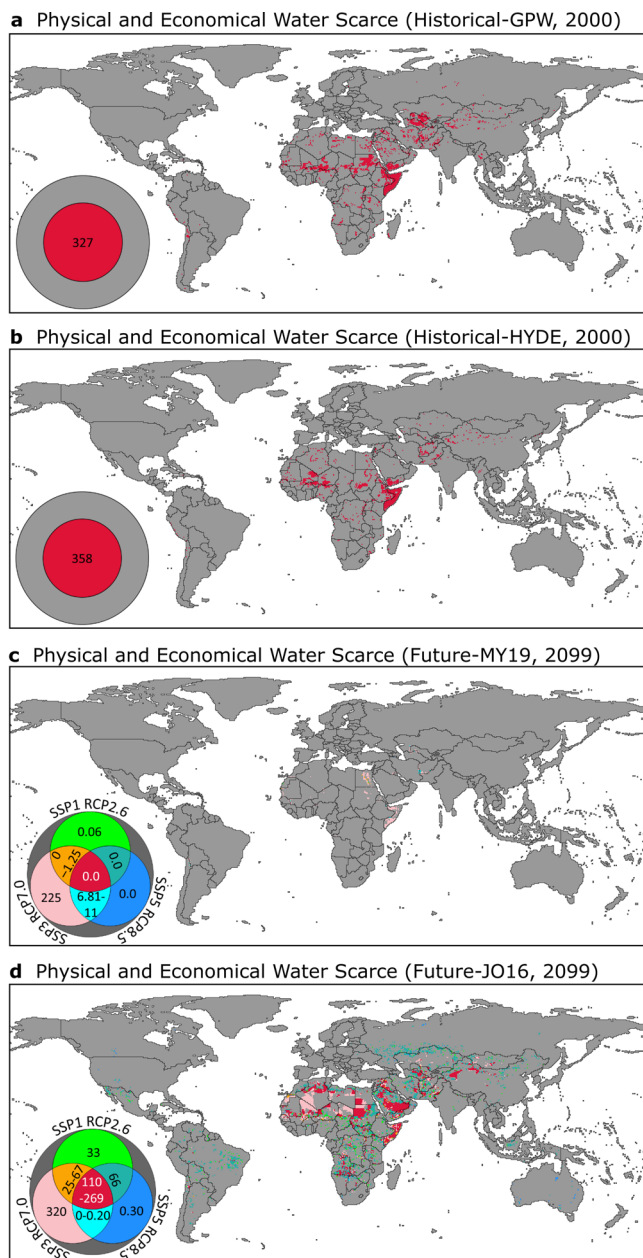


Fig. 3 Physical and economic water-scarce regions. **a** Historical (2000) considering the GPWv4 dataset, **(b)** Historical (2000) considering the HYDE3.2 population dataset, **(c)** Future (2099) considering the MY19 population dataset, and **(d)** Future (2099) considering the JO16 population dataset scenarios. The future (2099) case shows the possible combinations of scenarios with different colours; the values inside the circular legend show the number of people (in millions) facing scarcity with ranges representing the minimum and maximum values considering scenarios combination.

million (range shows the minimum and maximum population affected considering all three future scenarios), considering the historically available freshwater for future scenarios, i.e., Historical-MY (Historical-JO) experiments. Similarly, the population affected considering the historical population for the future scenarios, i.e., Future-GPW (Future-HYDE) experiments, was determined to be 13 (10–16) million; considering the historical GDP-PPP for the future scenarios, i.e., Future-MY-TG, (Future-JO-TG) experiments, the result was 1514–2928 (1466–3132) million (Supplementary Fig. 4 and Supplementary Fig. 5, Supplementary Table 7 for experiment

settings). The comparison of all sensitive analysis scenarios values with the base scenario value of 0.0 (110–269) million (Fig. 3c, d) showed that the effects of the different variables were in the order of GDP > population > climate for the regions with the highest chances of facing water scarcity in future.

Even though the overall water availability on the globe per capita are 6525.16 (6434.99) $\text{m}^3/\text{capita}/\text{year}$ for historical (i.e., the year 2000) and 6960.63 (6375.98) $\text{m}^3/\text{capita}/\text{year}$, and 3894.64 (3671.39) $\text{m}^3/\text{capita}/\text{year}$, 6821.34 (6459.90) $\text{m}^3/\text{capita}/\text{year}$ for future (i.e. the year 2099) considering SSP1-RCP2.6, SSP3-RCP7.0, and SSP5-RCP8.5 scenarios respectively (values in bracket consider HYDE3.2 and JO16 population datasets), more than 70% of world population faces the physical water scarcity defined using a threshold value of 1700 $\text{m}^3/\text{capita}/\text{year}$ of APC¹⁵ for all the scenarios (Supplementary Table 8, and Supplementary Note 1). Estimation of population facing severe water stress considering physical aspect only (i.e., APC of 500 $\text{m}^3/\text{capita}/\text{year}$) is 2.7 billion for historical scenarios and 3.9–7.9 (3.3–7.5) billion for the future scenario, whereas considering both physical and economic aspects (i.e., threshold line defined by Oki et al.¹⁹) is 301 (333) million for the historical scenarios and 0.33–325 (176–665) million for the future scenarios (Supplementary Fig. 6 and Supplementary Fig. 7). These values show a substantial difference in the water-stressed population when considering only physical aspects and accounting for both physical and economic factors. It also indicates that a few rich (i.e., grids with high GDP-PPP per capita) physical water-scarce regions (water-stressed regions identified using APC) can ease water scarcity by water management and technological measures.

The overall analysis revealed the possibility of underestimation (or overestimation) of the population facing scarcity in the future due to large differences associated with the population and GDP data distribution within the country for the SSP scenarios. The spatial distribution of the future population and GDP within and outside a country can be affected by many factors, such as water availability^{27,28}, job opportunities, disaster adaptation and mitigation capability of a location, migration of people²⁹, and different policies, which can be directly and indirectly associated with climatic^{29,30} and socioeconomic factors^{27,29}. Hence, it would be preferable for the projection of population and GDP to consider the feedback from the hydrological and hydrodynamic models to increase their reliability based on various climate phenomena, such as water availability, floods, and droughts, in addition to simple approaches such as the statistical model limited to roads and other infrastructure for auxiliary variables by Murakami and Yamagata²¹ and the gravity-based model by Jones and O'Neill²².

Conclusion

Country-level predictions of future water scarcity confirmed that no countries fell below the line expressed by Eq. 1, indicating no countries face both hydrological and economic difficult situations following the threshold line derived by Oki et al.¹⁹.

Grid-level analyses identified locations facing water scarcity that are unidentifiable at the country scale. The studies suggested that there will be a reduction in water scarcity for five of the six future scenarios considered due to an increase in income.

The analysis for the future considering urban concentrated (MY19) and dispersed (JO16) gridded population datasets confirmed large uncertainty of 169.1–338 million in the population facing water scarcity. This uncertainty is as considerable as the uncertainties of 6.58–489 million and 0.03–248 million associated with the SSP-RCP path in the future taken by the society and the climate models, respectively.

The study further confirmed the predominant effect of socio-economic factors (i.e., GDP and population) over climate-related

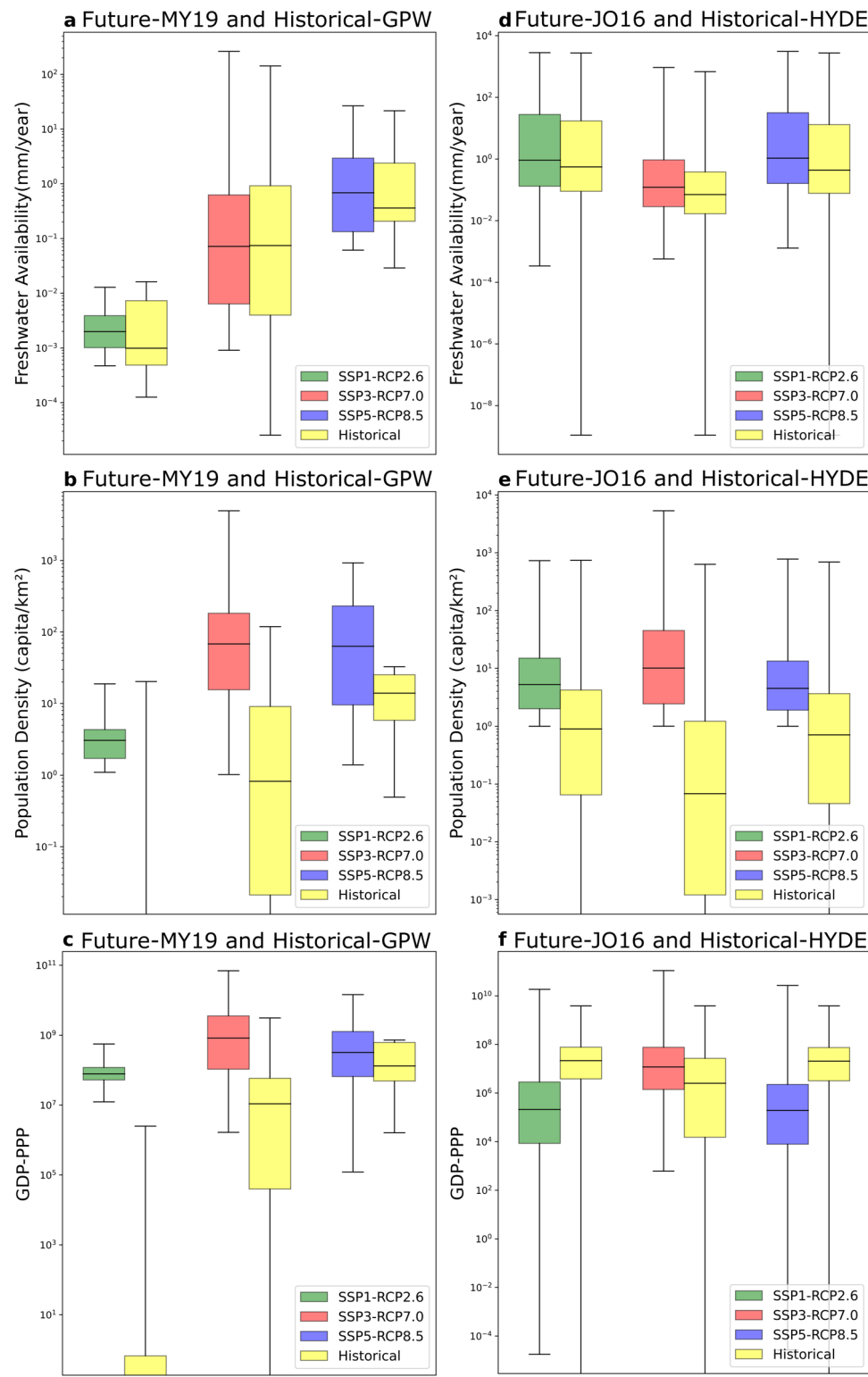


Fig. 4 Comparison of new water-scarce grids (i.e., grids facing physical and economic water scarcity in the future but not in the past). Box plots comparing the absolute values of (a), (d) freshwater availability (mm/year); (b), (e) population density (capita/km²); and (c), (f) GDP-PPP. The analysis for (a), (b), and (c) was performed considering the Future-MY and Historical-GPW Experiment settings, and that of (d), (e), and (f) was performed considering the Future-JO and Historical-HYDE experiment settings (Supplementary Table 1). The error bars show the 100% confidence interval (i.e., 0th and 100th percentile), the bottom and top of the box are the 25th and 75th percentiles, and the line inside the box is the median (50th percentile).

ones (i.e., available freshwater) for future water scarcity. Later indicating sufficient availability of freshwater for living on the globe and places with high economic potential can ease water scarcity with management and technological measures.

This study had certain limitations. We mainly used an empirical threshold line to define physical and economic water scarcity, assuming it is unchanged throughout the century. The top-down approach has limitations in reflecting local necessities and the availability of resources and services, which needs a bottom-up approach for assessment. We used GDP-PPP with the constant exchange rate of USD 2005, which has constraints in capturing the relative price change for the goods and services over the period³¹. We did not explicitly account for water use (e.g., sector-wise water withdrawal) or water management (e.g., virtual water trade), considering them only implicitly in GDP and population. Furthermore, the groundwater accounted in the runoff, assuming that groundwater recharge comes from baseflow. Similarly, environmental flow is implicitly included in the empirical threshold, assuming that the minimum threshold value of 500 m³/capita/year APC is substantial for non-irrigated areas. The analyses were limited to using a single water resources model (i.e., H08) to calculate runoff and water withdrawals. Additionally, we have reprojected the SSP5 country-level population and GDP to the grid level, assuming that the distribution within a country is identical to SSP1 of the MY19, which may have some limitations because SSP1 and SSP5 depict different world views³².

We demonstrated the importance of gridded data for future water scarcity assessments. The analysis showed considerable uncertainty in future water scarcity assessment due to the distributions of the gridded population within a country with magnitude in the scale of the uncertainty of extreme future scenarios. We examined future extremities by considering multiple GCMs, two gridded datasets, and future scenarios representing a world of sustainability (SSP1–RCP2.6), regional rivalry (SSP3–RCP7.0), and fossil fuel development (SSP5–RCP8.5), thus capturing the highest variation in the population exposed to water stress. Our findings will facilitate the development and implementation of policies and countermeasures, in advance, by displaying locations that will be more challenged by water scarcity in the future.

Methods

We primarily used river discharge (a proxy of water availability), population, and GDP data. We adopted the Shared Socioeconomic Pathways (SSP)³³ and the Representative Concentration Pathways (RCP)³⁴ frameworks for future projection. SSP describes the future evolution of society by examining how global society, demographics, and economics might change over the next century³⁵. RCP sets different levels of long-term climate stabilisation targets and depicts the greenhouse gas emissions path for each³⁵. We examined historical and future simulations under different scenario combinations of SSP and RCP (i.e., SSP1–RCP2.6, SSP3–RCP7.0, and SSP5–RCP8.5), which have been chosen by the Inter-Sectoral Impact Model Intercomparison Project Phase 3 (ISIMIP3; <https://www.isimip.org/>) protocol.

Global river discharge simulations. River discharge at the 0.5° grid level with a daily time scale was obtained using the H08 Global Hydrological Model^{36–38}. The simulations of H08 were performed using the ISIMIP 3a and ISIMIP 3b protocols for the historical period of 1901 to 2016 and the future period of 2015 to 2100. We used bias-corrected³⁹ observation-based (GSWP3–W5E5) climate data for the ISIMIP 3a and biased-corrected³⁹ CMIP 6 climate model, namely, GFDL-ESM4, IPSL-CM6ALR, MPI-ESM1–2HR, MRI-ESM2–0, and UKESM1–0–LL, data for ISIMIP 3b protocols corresponding to RCP 2.6, 7.0, and 8.5. Varying socio-economic scenario for the historical period as per the observed data and a fixed 2015 socioeconomic scenario for the future period were used for the H08 simulations.

Data for analyses. Historical population data at the beginning of the century (i.e., the year 2000) of the GPWv4⁴⁰ and HYDE3.2⁴¹ datasets, and the future population data of Murakami and Yamagata (MY19)²¹ and Jones and O'Neill (JO16)²² for the end of this century (i.e., the year 2099), were used for analyses. The GPWv4 dataset

is based on the area-weighted of observed data without any modelling consideration for spatialisation⁴². The HYDE3.2 datasets from 1950 to 2015 were developed considering United Nations World Populations Prospects (2008 Revision) using a combined weight layer based on soil suitability, road accessibility, distance from the water body, night light and other indicators to spatialise population data⁴². The MY19 data used the statistical downscaling method for population distribution producing a concentrated urban population. Its validation to GPW version 3²¹ (<http://sedac.ciesin.columbia.edu/>) showed high accuracy²¹, hence consistent with GPWv4. The JO16 gridded population dataset was developed considering GPW version 3²¹ using parameterised gravity-based downscaling approach producing a dispersed population. The national and state boundaries for the country-level analyses were derived from the 0.5° national identifier grid⁴³ (<http://sedac.ciesin.columbia.edu/>). As future population data of SSP5 are not included in MY19, we prepared them by scaling OECD-projected SSP5 future population data^{32,44} (<https://tntcat.iiasa.ac.at/SppDb/>) to the SSP1 distribution due to its closest resemblance in most of demographic components and assumptions for all country groupings⁴⁴.

We used the gridded GDP data of Geiger (hereafter TG18)²³ (Potsdam Institute for Climate Impact Research, Germany; <https://www.isimip.org/>) for the beginning of the century and those of MY19²¹ for the end of the century under SSP1 and SSP3. These data, available at 0.5° grid-scale, were used directly for analyses. Because those data for SSP5 were not available at grid-scale, we established such by assuming that the subnational distribution was identical to SSP1. The OECD-projected SSP5 future GDP data^{32,45} (<https://tntcat.iiasa.ac.at/SppDb/>) were distributed the same way as the SSP1 GDP provided by MY19.

Analyses for physical and economic water scarcity. The output data of H08 and the various other datasets, as explained above, were considered for the analyses. Historical variables as per the protocol were taken for analyses of the population affected due to the economy and water stress for the year 2000. The SSP1, SSP3, and SSP5 socioeconomic conditions, i.e., population and GDP along with the H08 outputs simulated for the RCP2.6, RCP7.0, and RCP8.5 climate conditions and 2015 socioeconomic conditions, were used to analyse the population challenged by physical and economic water stress at the end of the century. Thirty-year arithmetic means (i.e., 1971–2000 and 2070–2099) of daily discharge were used for analyses. The mean value was used to reduce the interannual variability. The annual GDP and population for the years 2000 and 2099 were specifically considered for the analyses as they are not affected by climate variability.

The physical water stress was calculated at the global scale using the availability per capita (APC)^{18,46} at the 0.5° grid-scale (~50 km resolution). The APC is estimated using mean annual discharge, defined by the sum of surface and subsurface runoff after routing, representing the renewable source of freshwater availability. Although the H08 hydrological model simulations considered the effects of dams, desalination plants, and larger transfer structures, the future projections of these were limited and restricted to the present scenario and the available data. Because the APC does not completely account for the capacity to use water¹², despite its availability and abundance and the other forms of available water such as import in terms of virtual water, its value represents the people challenged by physical water scarcity alone.

Economic water scarcity was quantified using the gross domestic product (GDP) per capita, an indicator of the development of a country's economy⁴⁷, with the help of an empirical equation showing the relationship between APC and GDP per capita, derived by Oki et al.¹⁹. The APC and GDP per capita relationship defined a threshold line given by the following expression:

$$\log \text{APC} = -2 \log \text{GPC} + 8, \quad (1)$$

where APC is in the unit of m³/capita/year and GPC is GDP per capita in the unit of USD/capita/year. The relationship is defined such that countries below the threshold line of $\text{APC} = 10^{(-2 \log_{10}(\text{GPC}) + 8)}$ face physical water scarcity and economic hardship (i.e., physical and economic water stress) simultaneously.

Oki and Quiocho²⁰ used the same relationship using per capita GDP considering purchasing power parity (GDP-PPP) with the exchange rate of USD 2005, quantifying physical and economic water scarcity at a resolution of ~50 km grid-scale to identify the economically challenged and water-scarcity regions at present. Here, we followed the same method, considering the multiple climate scenarios (observation-based historical climate and CMIP6 climate models) and socioeconomic scenarios, quantifying physical and economic water scarcity at the country scale and a resolution of 0.5° (~50 km) at the beginning and the end of the 21st century. We used GDP-PPP per capita (USD 2005) due to its availability for the past and future scenarios, and the same threshold line over the century to compare the absolute change in the water stress population and its spatial distribution.

We considered multiple sources of the population to show the effects of the distribution of population within the country on water scarcity. The analyses were first performed using the GPWv4 and MY19 datasets due to their consistency, i.e., Historical-GPW, Future126-MY19, Future370-MY19, and Future585-MY19 experiments (Supplementary Table 1 for experimental settings and data used in the analyses) and later performed using HYDE3.2 and JO16 datasets for comparison, i.e., Historical-HYDE, Future126-JO16, Future370-JO16, and Future585-JO16 (Supplementary Table 1). These experiments were treated as base scenario

experiments to be compared later with other experiments and scenarios. The result identified the locations with significant water stress and quantified the number of people affected in these regions. We performed Welch's two-sample *t*-test and Mood's median test considering the future scenarios and historical scenario datasets for APC and GPC for the country and grid-scale analyses. The statistical analyses were performed to compare the mean and median values of samples and their significance, represented by *p*-values.

New water-scarcity grids of the future, i.e., the grids facing water scarcity in the future but not having scarcity in the past, were analysed to determine the major factors making these grids water-scarce in the future. We compared the absolute value of available freshwater, population density, and GDP-PPP of new water-scarce grids (i.e., Future126-MY19, Future370-MY19, Future585-MY19, Future126-JO16, Future370-JO16, and Future585-JO16 experiments) with those of the past (i.e., Historical-GPW and Historical-HYDE experiments) to understand major contributing variable among the considered ones behind the water scarcity in these regions. Welch's two-sample *t*-test and Mood's median test for freshwater availability, population density, and GDP-PPP, comparing future and historical scenario grid values, were performed to compare the mean and median values of samples and their significance for water scarcity.

We also performed sensitivity analyses to determine the prevalent factors among climate, population, and GDP for water scarcity in the future for the whole world. These were performed using the historical scenario (i.e., the year 2000) freshwater availability, population, and GDP, considering one at a time and keeping other two variables of the future scenarios, i.e., future scenario of population and GDP, future scenario of freshwater availability and GDP, and future scenario of freshwater availability and population, respectively (Supplementary Table 7).

Data availability

GCMs data and the JO16 population dataset are available on the Inter-Sectoral Impact Model Intercomparison Project (ISIMIP) website (<https://www.isimip.org/>). The national and state boundaries and GPW4 population datasets are available on the Socioeconomic Data and Application Center (SEDAC) website (<http://sedac.ciesin.columbia.edu/>). The MY19 population and GDP datasets are available at the Center for Global Environmental Research (CGER), National Institute for Environmental Studies (<https://www.cger.nies.go.jp/gcp/population-and-gdp.html>). The OECD country-level population and GDP data are available on the International Institute for Applied Systems Analysis (IIASA) website (<https://tntcat.iiasa.ac.at/SspDb/>). Data used to support the study findings are available at <https://doi.org/10.5281/zenodo.6545219>.

Code availability

The H08 source code is available at <https://doi.org/10.5281/zenodo.4263375>. Code to produce all figures and source code for the analysis are available at <https://doi.org/10.5281/zenodo.6545261>.

Received: 16 November 2021; Accepted: 10 June 2022;

Published online: 25 June 2022

References

1. Oki, T. & Kanae, S. Global hydrological cycles and world water resources. *Science* **313**, 1068–1072 (2006).
2. Wada, Y., Van Beek, L. P. H., Wanders, N. & Bierkens, M. F. P. Human water consumption intensifies hydrological drought worldwide. *Environ. Res. Lett.* **8**, 034036 (2013).
3. Wada, Y. et al. Modeling global water use for the 21st century: The Water Futures and Solutions (WFaS) initiative and its approaches. *Geosci. Model Dev.* **9**, 175–222 (2016).
4. Vörösmarty, C. J., Green, P., Salisbury, J. & Lammers, R. B. Global water resources: vulnerability from climate change and population growth. *Science* **289**, 284–288 (2000).
5. Veldkamp, T. I. E. et al. Water scarcity hotspots travel downstream due to human interventions in the 20th and 21st century. *Nat. Commun.* **8**, 15697 (2017).
6. Shiklomanov, I. A. Appraisal and assessment of world water resources. *Water Int.* **25**, 11–32 (2000).
7. Falkenmark, M. Meeting water requirements of an expanding world population. *Philos. Trans. R. Soc. London. Ser. B: Biol. Sci.* **352**, 929–936 (1997).
8. Flörke, M. et al. Domestic and industrial water uses of the past 60 years as a mirror of socio-economic development: A global simulation study. *Glob. Environ. Chang.* **23**, 144–156 (2013).
9. Raskin, P., Gleick, P., Kirshen, P., Pontius, G. & Strzepek, K. *Water Futures: Assessment of Long-range Patterns and Problems. Comprehensive Assessment of the Freshwater Resources of the World* (SEI, 1997).
10. Jones, N. A drop to drink. *Nat. Clim. Chang.* **2**, 222–222 (2012).
11. Kummu, M. et al. The world's road to water scarcity: Shortage and stress in the 20th century and pathways towards sustainability. *Sci. Rep.* **6**, 1–16 (2016).
12. Rijsberman, F. R. Water scarcity: Fact or fiction? *Agric. Water Manag.* **80**, 5–22 (2006).
13. Hoekstra, A. Y., Mekonnen, M. M., Chapagain, A. K., Mathews, R. E. & Richter, B. D. Global monthly water scarcity: Blue water footprints versus blue water availability. *PLoS ONE* **7**, e32688 (2012).
14. Seckler, D., Barker, R. & Amarasinghe, U. Water scarcity in the twenty-first century. *Int. J. Water Resour. Dev.* **15**, 29–42 (1999).
15. Liu, J. et al. Water scarcity assessments in the past, present, and future. *Earth's Future* **5**, 545–559 (2017).
16. Kummu, M., Ward, P. J., De Moel, H. & Varis, O. Is physical water scarcity a new phenomenon? Global assessment of water shortage over the last two millennia. *Environ. Res. Lett.* **5**, 034006 (2010).
17. Fukuda, S., Noda, K. & Oki, T. How global targets on drinking water were developed and achieved. *Nat. Sustain.* **2**, 429–434 (2019).
18. Falkenmark, M., Lundqvist, J. & Widstrand, C. Macro-scale water scarcity requires micro-scale approaches. *Nat. Resour. Forum.* **13**, 258–267 (1989).
19. Oki, T., Yano, S. & Hanasaki, N. Economic aspects of virtual water trade. *Environ. Res. Lett.* **12**, 044002 (2017).
20. Oki, T. & Quiacho, R. E. Economically challenged and water scarce: identification of global populations most vulnerable to water crises. *Int. J. Water Resour. Dev.* **36**, 416–428 (2020).
21. Murakami, D. & Yamagata, Y. Estimation of gridded population and GDP scenarios with spatially explicit statistical downscaling. *Sustainability* **11**, 2106 (2019).
22. Jones, B. & O'Neill, B. C. Spatially explicit global population scenarios consistent with the Shared Socioeconomic Pathways. *Environ. Res. Lett.* **11**, 084003 (2016).
23. Geiger, T. Continuous national gross domestic product (GDP) time series for 195 countries: past observations (1850–2005) harmonized with future projections according to the Shared Socio-economic Pathways (2006–2100). *Earth Syst. Sci. Data* **10**, 847–856 (2018).
24. Somalia—The World Factbook. <https://www.cia.gov/the-world-factbook/countries/somalia/#economy>.
25. Benabdallah, K. The Position of the European Union on the Western Sahara Conflict. *J. Contemporary Eur. Stud.* **17**, 417–435 (2009).
26. San Martin, P. Nationalism, identity and citizenship in the Western Sahara. *J. North Afr. Stud.* **10**, 565–592 (2007).
27. Nagabhatla, N. et al. Water and migration: a global overview. *UNU-INWEH Rep. Ser.* **10**, 28 (2020). Issue.
28. Wrathall, D. J., Van Den Hoek, J., Walters, A. & Devenish, A. *Water Stress and Human Migration: a Global, Georeferenced Review of Empirical Research* (CABI, 2018).
29. McAuliffe, M. & Triandafyllidou, A. *World Migration Report 2022* (2021).
30. Biermann, F. & Boas, I. Preparing for a warmer world: towards a global governance system to protect climate refugees. *Glob. Environ. Polit.* **10**, 60–88 (2010).
31. Schreyer, P. & Koechlin, F. Purchasing power parities - measurement and uses. *Stat. Br.* **3**, 1–8 (2002).
32. Riahi, K. et al. The Shared Socioeconomic Pathways and their energy, land use, and greenhouse gas emissions implications: An overview. *Glob. Environ. Chang.* **42**, 153–168 (2017).
33. O'Neill, B. C. et al. A new scenario framework for climate change research: the concept of shared socioeconomic pathways. *Clim. Change* **122**, 387–400 (2014).
34. van Vuuren, D. P. et al. The representative concentration pathways: an overview. *Clim. Change* **109**, 5–31 (2011).
35. O'Neill, B. C. et al. Achievements and needs for the climate change scenario framework. *Nat. Clim. Chang.* **10**, 1074–1084 (2020).
36. Hanasaki, N. et al. An integrated model for the assessment of global water resources—Part 2: applications and assessments. *Hydrol. Earth Syst. Sci.* **12**, 1027–1037 (2008).
37. Hanasaki, N., Yoshikawa, S., Pokhrel, Y. & Kanae, S. A global hydrological simulation to specify the sources of water used by humans. *Hydrol. Earth Syst. Sci.* **22**, 789–817 (2018).
38. Hanasaki, N., Yoshikawa, S., Pokhrel, Y. & Kanae, S. A quantitative investigation of the thresholds for two conventional water scarcity indicators using a state-of-the-art global hydrological model with human activities. *Water Resour. Res.* **54**, 8279–8294 (2018).
39. Lange, S. Trend-preserving bias adjustment and statistical downscaling with ISIMIP3BASD (v1.0). *Geosci. Model Dev.* **12**, 3055–3070 (2019).
40. University, C. for I. E. S. I. N.-C.-C. Gridded Population of the World, Version 4 (GPW4): Population Count, Revision 11 <https://doi.org/10.7927/H4JW8BX5> (2018).

41. Klein Goldewijk, K., Beusen, A., Doelman, J. & Stehfest, E. Anthropogenic land use estimates for the Holocene—HYDE 3.2. *Earth Syst. Sci. Data* **9**, 927–953 (2017).
42. Chen, R., Yan, H., Liu, F., Du, W. & Yang, Y. Multiple global population datasets: Differences and spatial distribution characteristics. *ISPRS Int. J. Geo-Information* **9**, 637 (2020).
43. University, C. for I. E. S. I. N.-C.-C. Gridded Population of the World, Version 4 (GPWv4): National Identifier Grid, Revision 11 <https://doi.org/10.7927/H4TD9VDP> (2018).
44. KC, S. & Lutz, W. The human core of the shared socioeconomic pathways: Population scenarios by age, sex and level of education for all countries to 2100. *Glob. Environ. Chang* **42**, 181–192 (2017).
45. Dellink, R., Chateau, J., Lanzi, E. & Magné, B. Long-term economic growth projections in the Shared Socioeconomic Pathways. *Glob. Environ. Chang* **42**, 200–214 (2017).
46. Shiklomanov, I. A. *Assessment of Water Resources and Water Availability in the World* 88 (World Meteorological Organization, 1997).
47. Kummu, M., Taka, M. & Guillaume, J. H. A. Gridded global datasets for Gross Domestic Product and Human Development Index over 1990–2015. *Sci. Data* **5**, 1–15 (2018).

Acknowledgements

This research was funded by the Japan Society for the Promotion of Science [KAKENHI], grant numbers 16H06291 and 21H05002, and the Environment Research and Technology Development Fund of the Environmental Restoration and Conservation Agency of Japan, grant number JPMEERF20202005. The author is thankful to JICA (Japan International Cooperation Agency) for supporting this research.

Author contributions

P.M. investigated the research, performed the analysis, and wrote the manuscript, T.O. conceptualised the research, N.H. and D.Y. helped in the writing and finalisation of the manuscript, J.E.S.B. performed the H08 simulations.

Competing interests

The authors declare no competing interests.

Additional information

Supplementary information The online version contains supplementary material available at <https://doi.org/10.1038/s43247-022-00475-w>.

Correspondence and requests for materials should be addressed to Prakat Modi.

Peer review information *Communications Earth & Environment* thanks Alexander Horton and the other, anonymous, reviewer(s) for their contribution to the peer review of this work. Primary Handling Editors: Alessandro Rubino, Joe Aslin, Clare Davis.

Reprints and permission information is available at <http://www.nature.com/reprints>

Publisher's note Springer Nature remains neutral with regard to jurisdictional claims in published maps and institutional affiliations.



Open Access This article is licensed under a Creative Commons Attribution 4.0 International License, which permits use, sharing, adaptation, distribution and reproduction in any medium or format, as long as you give appropriate credit to the original author(s) and the source, provide a link to the Creative Commons license, and indicate if changes were made. The images or other third party material in this article are included in the article's Creative Commons license, unless indicated otherwise in a credit line to the material. If material is not included in the article's Creative Commons license and your intended use is not permitted by statutory regulation or exceeds the permitted use, you will need to obtain permission directly from the copyright holder. To view a copy of this license, visit <http://creativecommons.org/licenses/by/4.0/>.

© The Author(s) 2022